NDT of austenitic steels – Evaluation of spot weld nugget diameters by imaging analyses of the residual magnetic flux density

Journal:	*12th European Conference on Non-Destructive Testing (12th ECNDT)*
Manuscript ID	ECNDT-0478-2018.R2
Type:	Abstract
Date Submitted by the Author:	n/a
Complete List of Authors:	Mathiszik, Christian; Technische Universitat Dresden Fakultat Maschinenwesen, Chair of Joining Technology and Assembly Reinhardt, Till; Technische Universitat Dresden Fakultat Maschinenwesen, Chair of Joining Technology and Assembly
Keywords:	Magnetic methods, Welds, Stainless steel, Metals, Quality control, Research

NDT of austenitic steels – Evaluation of spot weld nugget diameters by imaging analyses of the residual magnetic flux density

Christian Mathiszik, Till Reinhardt, Jörg Zschetzsche and Uwe Füssel

Technische Universität Dresden, Chair of Joining Technology and Assembly, Germany, christian.mathiszik@tu-dresden.de

Abstract

Non-destructive testing (NDT) of resistance spot welding compounds continues to pose a great challenge. The nugget diameter is the most important quality criterion. Established ultrasonic-based methods reach their limits when evaluating the nugget diameter of combinations with significantly different sheet thicknesses and with deep electrode indentations. In these cases, the imaging analysis of residual flux density shows high potential. Previous results of this NDT method concentrate on spot weld combinations of ferromagnetic steels. Hence, latest research at Technische Universität Dresden focuses on the application of the imaging analysis of residual magnetic flux density on spot welds using austenitic steels. Due to the high cooling rates after welding delta ferrite with ferromagnetic properties is generated inside the nugget, and therefore the residual magnetic flux density can be measured.

The talk will show the measuring concept of the NDT method for spot welds and presents the results of its application on two and three sheet metal combinations of austenitic steels.

1. Introduction

Conventional resistance spot welding of steel alloys is used to join two or more overlapping sheet metals. The sheet metals are between two copper electrodes. The electrodes have a much lower specific resistance than the sheet metals. The welding process consist of three main parts: squeeze time t_s, weld time t_w and hold time t_h. During the squeeze time the electrodes press the sheet metals with a defined force F_{el} together. Subsequently the welding current I_w introduced via the electrodes flows through the sheet metals. The contact and material resistance lead to a conductive heating until the base material melts. The heating can be described by Joule's first law (equation 1). After the welding current is switched off, the electrodes keep pressing the sheet metals and the weld to prevent defects of the weld like pores. Figure 1 shows a schematic cross-sectional view of a spot weld. A typical spot weld is characterized by a nugget, which was the molten material during the welding process, and the heat affected zone (HAZ) surrounding the nugget. Due to the high electrode forces F_{el}, the surface of a spot weld usually shows an electrode indentation on both sides. The main dimensions of the spot weld are not visible from outside and therefore not directly measurable. This applies in particular to the nugget diameter d_n, measured in the joint plane (JP) between the welded sheet metals, which is one of the most important quality criteria of a spot weld. Measuring the nugget diameter d_n still poses a great challenge for different NDT methods including established ultrasonic-based methods. According to DVS-2916-5 [1] these methods reach their limits when evaluating the nugget diameter of combinations with significantly different sheet thicknesses and with deep electrode indentations. In these cases, the imaging analysis of the residual magnetic flux density B_r of the spot weld, developed at the Technische Universität Dresden, shows high potential. With this method the spot weld is magnetized and the residual magnetic flux density is measured afterwards. Previous investigations of this NDT method concentrated on spot weld combinations of ferromagnetic steels (research project IGF 17.539 BR [2, 3]). The application of this method on combinations of austenitic steels are part of the current research project IGF 19.208 BR. The investigations are carried out on two and three sheet metal combinations of the austenitic steel 1.4301 (X5CrNi18-10) and will be discussed in this article. This steel alloy has a very wide range of application not only because of its good corrosion-resistant and good processing properties, also the attractive appearance is a factor. Examples for the usage are food production, processing and transportation, kitchen utensils, pipes etc.

$$Q = \int I^2 R \, dt \tag{1}$$

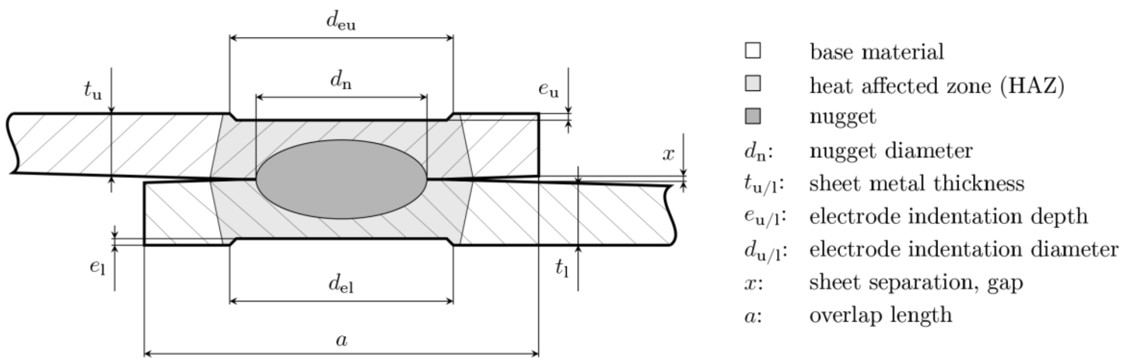

Figure 1. Schematic cross-sectional view of a resistance spot weld

2. Experimental setup and measuring concept

A detailed list of the material combinations (MC) for the investigations is shown in Table 1. The samples were welded with constant welding time t_w and electrode force F_{el} using a medium-frequency inverter. The different sizes of the nuggets were realized by varying the welding current I_w with three process parameter sets (PS1, PS2 and PS3).

Table 1. Investigated material combinations

test name	material combination	electrode force F_{el} /kN	welding time t_w /ms	welding current I_w /kA		
				PS1	PS2	PS3
11	1.4301 (1 mm) 1.4301 (1 mm)	3,5	220	3,6	5,6	7,6
22	1.4301 (2 mm) 1.4301 (2 mm)		250	3,4	5,4	7,4
122	1.4301 (1 mm) 1.4301 (2 mm) 1.4301 (2 mm)		300	3,2	5,2	7,2

The experimental setup is the same as used in [3]. The testing procedure of the imaging analysis of the residual magnetic flux density consists of two steps. Figure 2 shows both steps with the experimental setup. In the first step the sample with its weld is coaxially located between two coils oriented in the same direction and gets magnetized. Each coil has 133 windings and a magnetic core of the steel alloy S235 with a diameter of 16 mm. The magnetic field strength is adjusted so that the material reaches its magnetic saturation.

The magnetization time is less than 100 ms and the coils are removed afterwards. The residual magnetic flux density B_r is measured on the surface by scanning across the joint of the sample with a single Hall-sensor A1324 from Allegro Systems in the second step. Depending on the scanning resolution, one measurement takes about 4 minutes with this measurement setup of the TU-Dresden. Using the magnetic field camera Magcam Minicube1D the measurement time is less than 20 seconds. The Minicube1D has an integrated 2D Hall-sensor array of 128 x 128 magnetic field sensors on one single chip with a size of 12,7 mm x 12,7 mm [4]. All measurements are carried out on both sides of each sample. The result of the measurement can be analyzed using intensity charts. To evaluate the results of all measurements, each sample is destroyed by chisel test afterwards and the nugget diameter is measured according to DIN EN ISO 14329 [5].

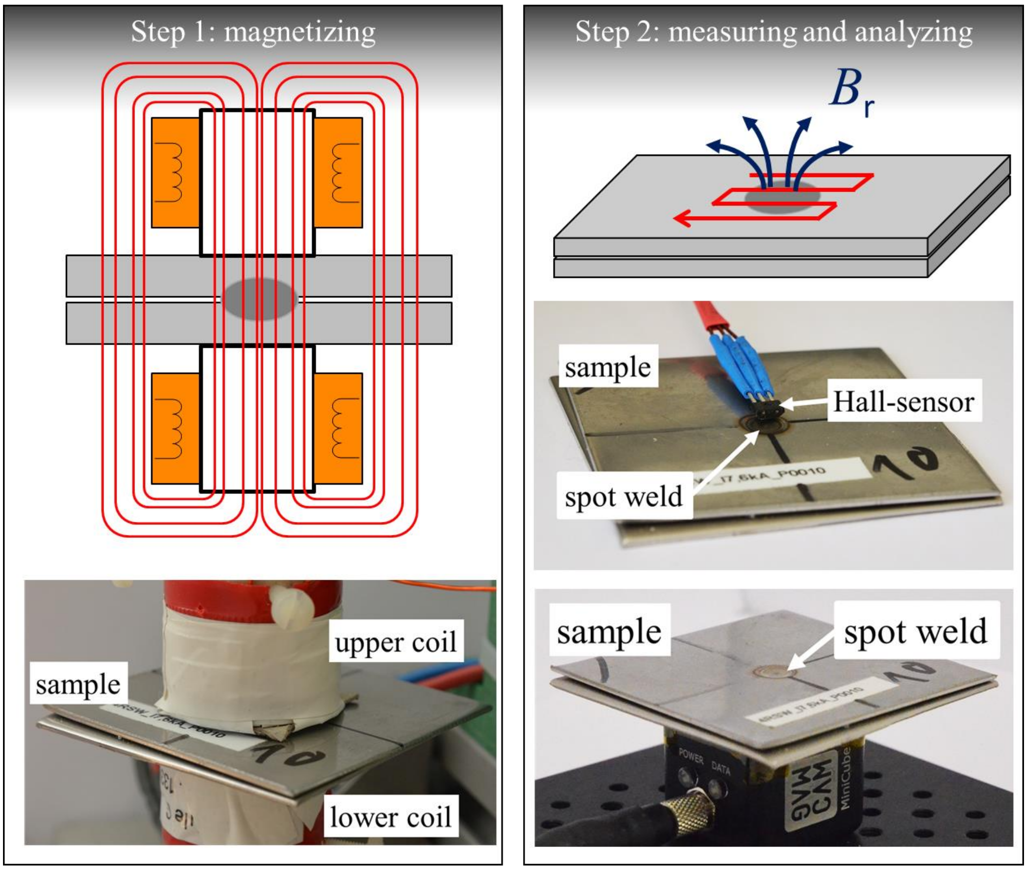

Figure 2. Testing procedure and experimental setup with magnetizing coils, Hall-sensor and Magcam Minicube1D

The evaluation of the measurements is done via a self-developed data processing algorithm. As it can be seen in Figure 3, the amount of the residual magnetic flus density in the welded and unwelded area is clearly different. At the edge of the weld nugget the amount of the residual magnetic flus density increases sharply. The first derivative of the magnetic flux density shows the maxima of this increase. The edge of the nugget in the JP can be detected where the second derivative equals zero (equations 2) (Figure 3c, d, light blue ring between the two red rings). From the enclosed area the mean diameter is calculated to determine the nugget size.

$$\Delta B_z = \frac{\partial^2 B_z}{\partial x^2} + \frac{\partial^2 B_z}{\partial y^2} = 0 \qquad (2)$$

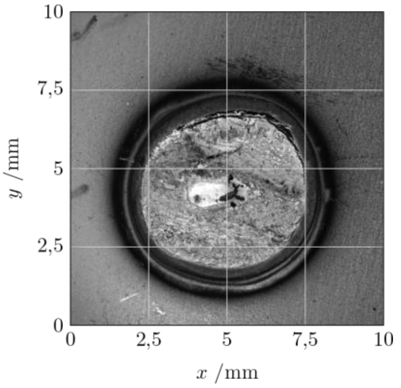

a) spot weld after destructive testing

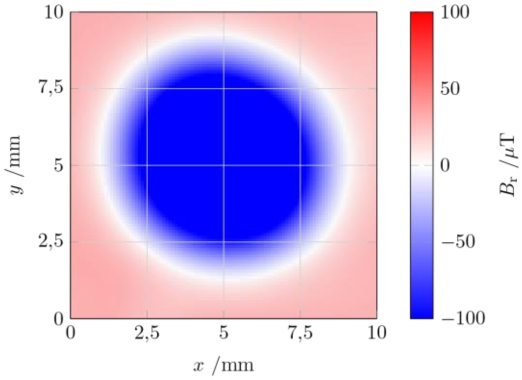

b) NDT of spot weld, raw data

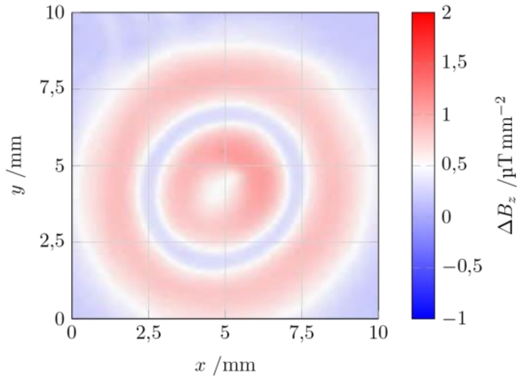

c) NDT of spot weld, 2. derivation

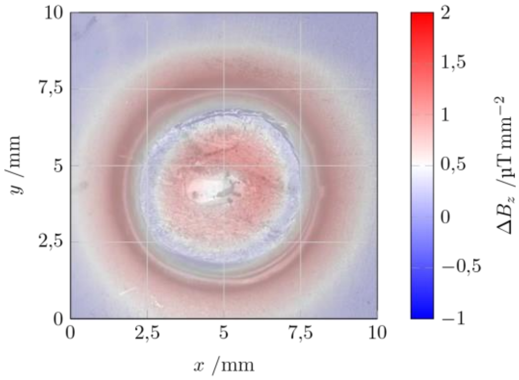

d) NDT of spot weld, 2. derivation, overlay with destructive testing (true to scale)

Figure 3. Comparison and overlay of a destroyed sample with the NDT measurement results and analysis algorithm

3. Results and discussion

The existence of the spot weld nugget can be clearly detected using the imaging analysis of the residual magnetic flux density as shown in Figure 4. A good weld shows a much higher amount of the residual magnetic flux density B_r caused by the nugget, whereas a poor weld or a stick weld show almost no difference between the weld area and the surrounding material. The NDT results of all samples compared with the destructive testing results are shown in Figure 5. The diameter d_p and the area A_p of the destructive testing tends to be larger in proportion to the diameter d_n and the area A_n of the nugget evaluated by NDT. This is a common appearance of the spot welding process [6].

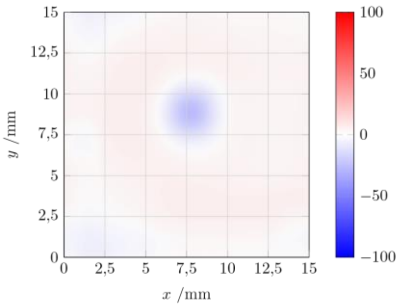

a) Stick weld without a nugget

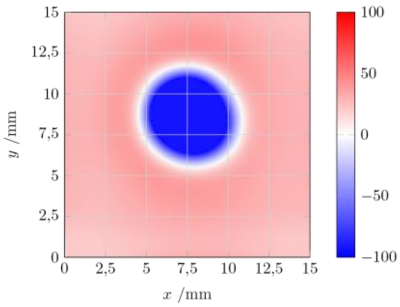

b) Good weld with a nugget diameter of 5,00 mm

Figure 4. Different NDT measurement results cause by different spot welding qualities

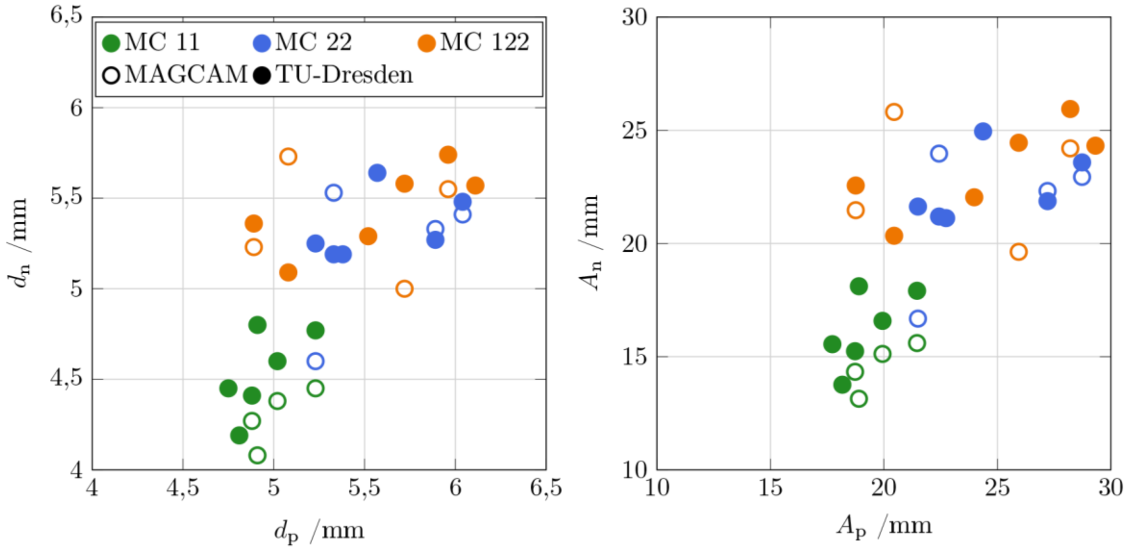

a) Comparison between the diameters of destructive testing and NDT

b) Comparison between the areas of destructive testing and NDT

Figure 5. Comparison of destructive testing (d_p, A_p) vs. NDT (d_n, A_n) used the experimental setup with Hall-sensor (TU-Dresden) and the magnetic field camera Magcam Minicube1D (MAGCAM)

The reason why the imaging analysis of the residual magnetic flux density works on spot welds with the austenitic steel 1.4301 can be declared by the characteristics of the spot welding process. Figure 6 shows a simulated spot welding process of the MC 11, PS3 with the temperature development and distribution. The software SORPAS 2D R12.5 was used for this simulation. The electrode force F_{el}, welding current I_w and the temperature curve of the nugget center (Node N320 in Figure 6b) are shown in Figure 6a. The cooling rate during the hold time t_h after spot welding is very high. An example of the temperature rate distribution after 100 ms of the hold time t_h (Point A) is illustrated in Figure 6b. The results of the simulation show cooling rates with an absolute amount of more than 1000 K/s in the welding area. These temperature rates are characteristic for spot welding processes and correlate with previous investigations in [7].

Considering the microstructure of the welds shown in Figure 7, the base material, the HAZ and the nugget differ significantly. 1.4301 belongs to the metastable austenitic steel and solidifies primarily to δ-ferrite [8]. While austenite has paramagnetic properties, δ-ferrite shows a ferromagnetic behavior. Due to the high cooling rates of the spot welding process, the structure does not have enough time to convert completely into austenite. Thus the nugget consists of a much higher proportion of δ-ferrite than the base material and the HAZ. After magnetizing the spot weld the higher amount of δ-ferrite of the nugget leads to a significantly higher residual magnetic flux density compared to the surrounding material. This measurable difference allows the evaluation of the nugget and can be used for non-destructive quality control.

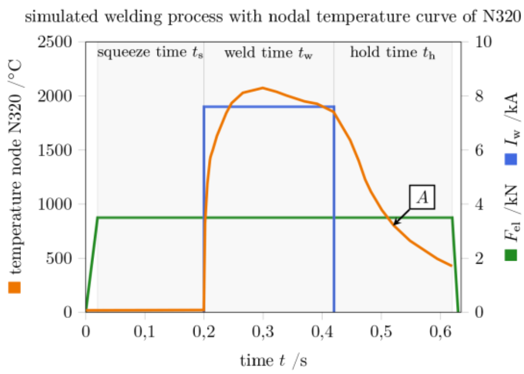

a) simulated welding process with the temperature curve of node N320

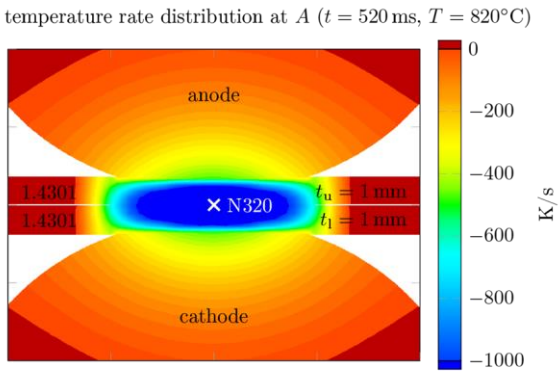

b) temperature rate distribution at A (t = 520 ms, T = 820°C)

Figure 6. Temperature development and rate distribution of the welding process of MC 11, PS3 simulated with SORPAS 2D R12.5 (F_{el} = 3,5 kN, t_w = 220 ms, I_w = 7,6 kA)

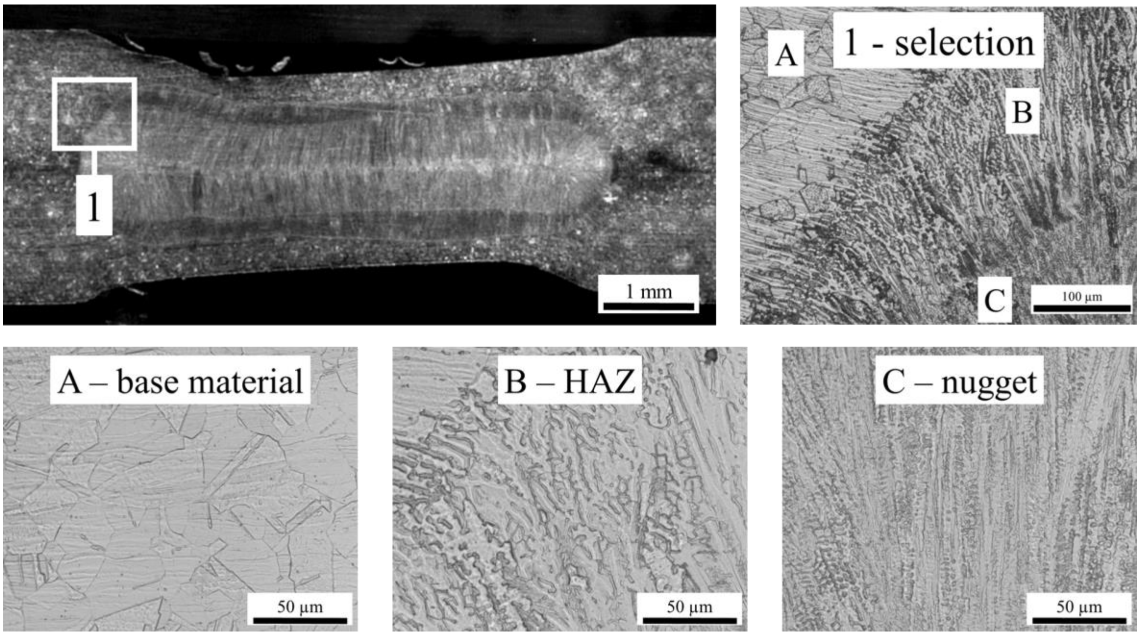

Figure 7. Microstructure of a spot weld with two 1.4301 (1,5 mm) (pictures taken by [9])

4. Conclusions

The application of the imaging analysis of the residual magnetic flux density on spot weld combinations with the austenitic steel 1.4301 shows good correlations between NDT and destructive testing. Currently the analysis algorithm is being improved. This will include an automated evaluation feature to reduce the influence of the testing personal. The characteristics of the spot welding process with its high cooling rates and the material behavior are the reason for these good results. This demonstrates that the field of application of this NDT method is not restricted on ferromagnetic steels only.

Acknowledgements

Das IGF-Vorhaben IGF 19.208 B/DVS-Nr. 04.070 der Forschungsvereinigung „Forschungsvereinigung Schweißen und verwandte Verfahren des DVS, Aachener Straße 172, 40223 Düsseldorf“ wurde über die AiF im Rahmen des Programmes zur Förderung der industriellen Gemeinschaftsforschung und -entwicklung (IGF) vom Bundesministerium für Wirtschaft und Energie aufgrund eines Beschlusses des Deutschen Bundestages gefördert.

Gefördert durch:
Bundesministerium für Wirtschaft und Energie
aufgrund eines Beschlusses des Deutschen Bundestages

The authors thank AiF for funding the IGF-Project IGF 19.208 BR of the Research Association on Welding and Allied Processes of the DVS, which was part of the program to support cooperative industrial research (Industrielle Gemeinschaftsförderung (IGF)) by the Federal Ministry of Economy and Energy, following a decision of the German Bundestag. Equal thanks go to all companies and participants, who contributed their support and knowledge to the project.

References

1. DVS Media GmbH, DVS 2916-5:2017-09, "Prüfen von Widerstandspressschweißverbindungen - Zerstörungsfreie Prüfung von Punktschweißverbindungen", DVS Media, 2017.
2. U Füssel, C Mathiszik, J Zschetzsche, C Großmann and M Heide, "Zerstörungsfreie Bewertung des Linsendurchmessers beim Widerstandspunktschweißen mit magnetischen Prüfverfahren", *research report IGF-Nr. 17.539 BR/DVS-Nr. 04.058*, Technische Universität Dresden, Chair of Joining Technology and Assembly, 2015.
3. C Mathiszik, J Zschetzsche, C Großmann and U Füssel, “Remanent Magnetization for Non-Destructive Testing of Spot Welds” in *DGZfP-Proceedings BB*, 158-USB, *19th WCNDT 2016 in Munich, Germany: Proceedings*, Munich, 2016.
4. Magcam NV, “Magcam Brochure: advanced magnet inspection”, 2017.
5. DIN Deutsches Institut für Normung e.V., DIN EN ISO 14329:2003-12, "Widerstandsschweißen - Zerstörende Prüfung von Schweißverbindungen - Brucharten und geometrische Messgrößen für Widerstandspunkt-, Rollennaht- und Buckelschweißungen", Beuth Verlag, 2003.
6. DVS Media GmbH, DVS 2902-3:2016-02, "Widerstandpunktschweißen von Stählen bis 3 mm Einzelblechdicke: Konstruktion und Berechnung", DVS Media, 2016.
7. Z Han, J Orozco, JE Indacochea and CH Chen, “Resistance Spot Welding: A Heat Transfer Study: Real and simulated welds were used to develop a model for predicting temperature distribution”, *Welding journal*, no. 68, 363s–371s, 1989.
8. G Schulze, "Die Metallurgie des Schweißens: Eisenwerkstoffe - Nichteisenmetallische Werkstoffe", 4th ed., Berlin, Heidelberg, Springer-Verlag, 2010.
9. C Halisch, C Mathiszik, J Zschetzsche and U Füssel, “Untersuchung der Veränderung magnetischer Eigenschaften des Werkstoffs während des Widerstandspunkschweißens” Interdisziplinäre Projektarbeit, Chair of Joining Technology and Assembly, Technische Universität Dresden, Dresden, 2016.